Comparison of the performance of a cylindrical Hall thruster with different anode voltages via numerical simulations

Sergio T. T. S. Junior[1], Rodrigo A. Miranda[1], Sarah G. S. P. Costa [1] and Helbert O. C. Júnior [1]

[1]*Faculty of Gama, University of Brasilia*
St. Leste Projeção A - Gama Leste, 72444-240, Brasilia-DF, Brazil
sergiojunior@unb.br, rmiracer@unb.br

Abstract. Plasma propulsion, or electric propulsion, arises from the need to explore deep space more economically and efficiently. The Cylindrical Hall Thruster (CHT) demonstrates enhanced propellant utilization and performance efficiencies within reduced dimensions and lower power thresholds when compared to conventional plasma propulsion devices. The compact size and operation at lower power levels make it an interesting option to provide propulsion for CubeSats and small satellites. The CHT comprises a channel with an annular anode through which neutral gas is injected, subsequently ionized by magnetized electrons injected from an external hollow cathode. The resulting plasma ions are ejected from the device, giving thrust. In this paper we perform numerical simulations of the CHT operating at two different potential values at the anode, namely, 150 V and 300 V. These two simulations are compared in terms of performance parameters such as thrust, specific impulse and efficiency. The numerical results obtained with this simplified model will allow to obtain an optimal configuration for a future prototype to be implemented at the Plasma Physics Laboratory at the University of Brasilia.

Keywords: CubeSats, Electric propulsion, Plasma, Ions.

1 Introduction

The search for new technologies aimed at efficiently exploring deep space has been increasingly studied. The aerospace industry has, for the most part, used chemical propulsion, which provides from a high amount of energy and a thrust sufficiently capable of overcoming the drag and weight forces, thus allowing space equipment to reach Earth orbit and even other planets [1]. However, one limitation of this type of propulsion is that, in order to launch a certain device, a high cost of fuel and oxidizer is necessary, in addition to significant storage space. These factors not only drive up expenses but also hinder the further advancement of space programs, impeding the realization of ambitious exploration objectives [1].

Electric propulsion emerged as a promising alternative to chemical propulsion in the mid-1950s [1]. Hall Thrusters (HTs) are electric propulsion devices, depending on the $\mathbf{E} \times \mathbf{B}$ effect, where $\mathbf{E}$ represents the electric field and $\mathbf{B}$ the magnetic field, resulting in a current known as the Hall current. Hall thrusters are capable of accelerating ions to high speeds [1], and have been extensively studied using computational methods.

The Cylindrical Hall Thruster (CHT) represents an alternative HT design that comprises a cylindrical region and a short annular channel. The CHT demonstrates improved propellant utilization and performance when compared to HTs. The magnetic field can be adjusted using electromagnet coils or permanent magnets. This device has applicability for micro and nano-satellites because this device can offer a higher ionization efficiency and silent operation, offering a better volume-to-surface ratio compared to compact HTs, potentially mitigating wall erosion [2, 3].

The CHT works by first filling a cylindrical chamber with neutral gas, with a small ring-shaped annular region near the surface of the anode. The non-magnetized ions are accelerated in the cylindrical channel by a potent electric field generated by the anode. Previous studies on the structure of this geometry assert that CHTs reduce the interaction between the plasma and the dielectric wall channel, electron transport, heat, and wall erosion [4].

In this paper we perform numerical simulations of a hybrid model of a cylindrical Hall thruster. We compare the performance of this thruster using two different values of the anode potential, namely, 150 V and 300 V. This paper is organized as follows. Section 2 describes the computational tools employed in this work. Section 3 presents the results from the numerical simulations. The conclusions are given in Section 4.

2 Computational methods

We employ the Finite Element Method Magnetics (FEMM) software to compute the magnetic field due to the permanent magnets. The simulations were performed in a two-dimensional (2D) domain, keeping the axial and radial directions, and ignoring variations in the azimuthal direction. Figure˜1 shows the simulation domain defined in the FEMM softwre. The vertical axis corresponds to the axial direction, and the geometry is symmetric around this axis. The position of the samarium-cobalt magnets are indicated by rectangles labelled by SmCo36, and their polarization is indicated by a small arrow. Regions marked as "Air" represent empty space. The contours between adjacent "Air" regions are defined for controlling the number of finite elements inside each region, and do not represent solid boundaries. The boundary of the simulation domain has a semicircular shape, and is set to Dirichlet conditions.

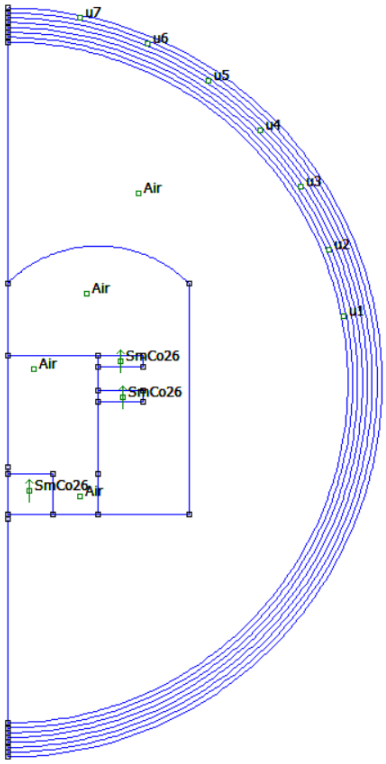

Figure 1. Simulation domain defined in the FEMM software, showing the position of the permanent magnets, marked as "SmCo36".

For the simulation of the plasma inside the channel, we use the Hall Ion Sources Simulation Software (HALLIS) which is a hybrid code developed at the LAPLACE laboratory [5]. The HALLIS software includes two autonomous modules for performing 1D e and 2D simulations, using a hybrid model for the plasma. In this model, electrons are treated as a fluid and neutral atoms are represented by pseudo-particles [6]. The simulations start by injecting xenon neutral gas intro the cylindrical chamber, resulting in a distribution density of neutrals inside the channel. The trajectories of positive ions and neutral atoms are computed through the integration of the equations of motion, considering collisions and interactions with walls (specular or diffusive). The transport of electrons across the magnetic barrier is described by empirical coefficients for the effective mobility and energy losses.

In this paper, were examine two different values of the electric potential, namely, 150V and 300V. Table 1 shows the numerical values of the simulation parameters of the HALLIS software. For each value of the anode potential, simulation results were recorded at three time, $t_1 = 450\ \mu s$, $t_2 = 500\ \mu s$, $t_3 = 550\ \mu s$. After obtaining the analyzed data for each moment, an average was calculated for a better visualization of the results.

3 Simulation results

3.1 Magnetic field simulations

Figure 2(a) shows the grid of finite elements needed for the calculation of the magnetic field due to the permanent magnets. Figure 2(b) shows the resulting magnetic field lines, which extend from the positions of the

permanent magnets, and their shapes depend on the polarization as defined in Fig. 1.

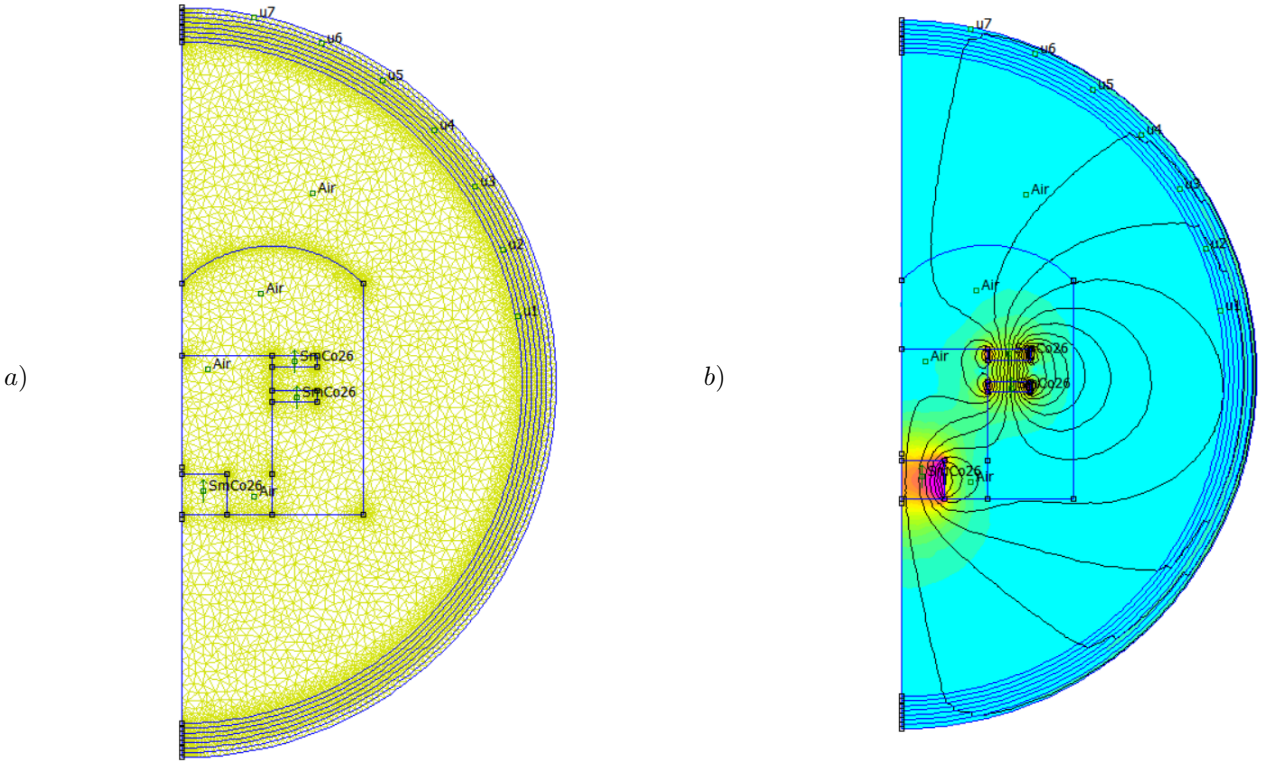

Figure 2. (a) Mesh used by FEMM with 11814 nodes. (b) FEMM magnetic density flux lines.

Table 1. Numerical values of the simulation parameters with the HALLIS software.

Parameters	**Values (cm)**
Axial domain	5.00
Radial domain	2.50
Channel Lenght	2.50
Inner Radius	0.00
Outer Radius	2.00
Cathode position	(2.50, 1.00)
Anode	(0.00 , 1.50)
Gas inlet	(1.25, 1.75)
Gas flow rate	5.0 mg/s
Gas temperature	500 K

3.2 Plasma simulations

In this section we compute the resulting plasma density and electric potential using two values of the electrostatic potential at the anode, namely, 150 V and 300 V. The magnetic field computed using the FEMM software and imported into the HALLIS software is depicted in Figure 3. The modulus of the magnetic field is represented in a color scale and displays variations in the axial (X) and radial (Y) directions of the channel. Note that the field lines concentrate closer to the location of the permanent magnets, which is also a region with higher magnetic field strength.

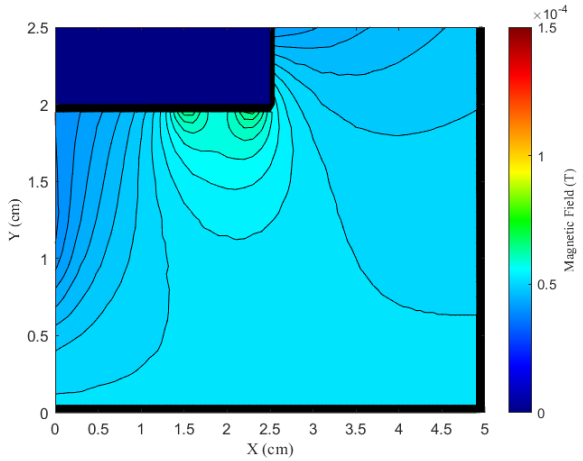

Figure 3. The magnetic field lines and the modulus of the magnetic field in color scale.

Figure 4 shows the results for an anode potential of 150 V. The electrostatic potential has a maximum value near the anode and decreases rapidly in the axial direction toward the channel exit region. The plasma density displays large values near the $Y = 0$ central axis of the channel. However, a localized maximum can be also distinguished towards the anode. This isolated maximum is due to a population of electrons trapped by the magnetic field colliding with the neutral gas, causing an enhancement of ionization and higher plasma density values.

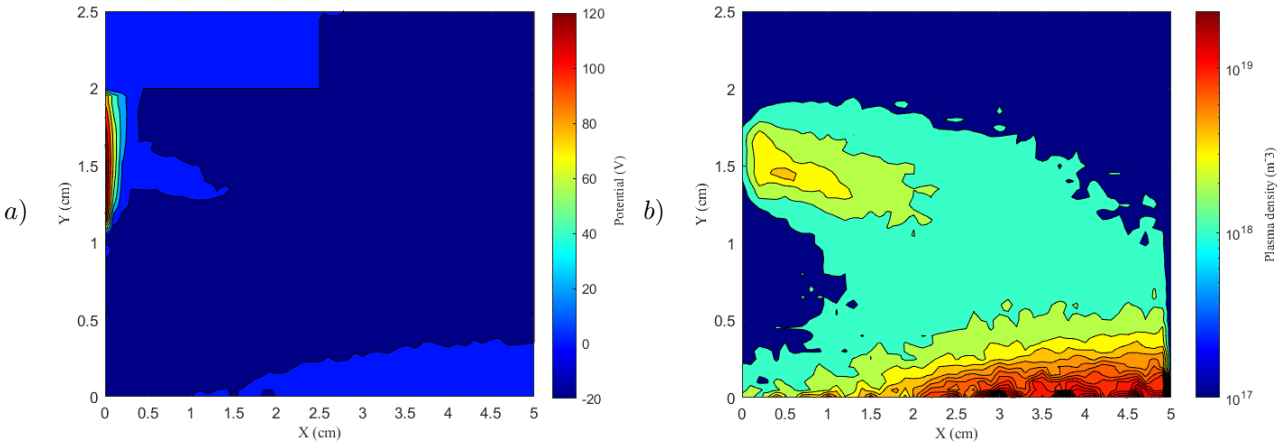

Figure 4. Contour plots of (a) the electrostatic potential, and (b) plasma density, for 150 V.

Following that, the anode potential was adjusted to a value of 300V keeping all other parameters fixed. Figure 5(a) shows that the electrostatic potential displays a similar pattern with the 150 V case. However, a narrow strip of low values extending from the anode to the channel exit can be observed.The plasma density also indicates the presence of a narrow strip linking the anode region to the central region at the channel exit, where the highest values are observed. Evidently, the higher potential value at the anode can increase the ionization rate near the anode, due to a higher number of electrons trapped in that region where the magnetic field is stronger (see Fig. 3).

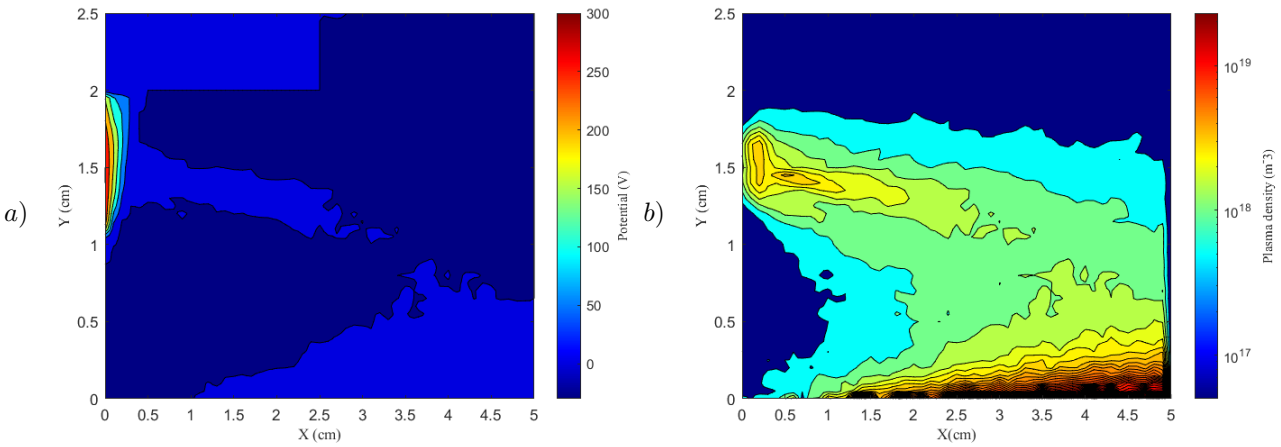

Figure 5. Contour plots of (a) the electrostatic potential, and (b) plasma density, for 300 V.

The performance of plasma thrusters can be evaluated by operational parameters such as thrust, specific impulse (I_{sp}), and efficiency (η). The thrust in this type of propulsion systems has units of millinewtons, and can be written by

$$T = -v_{ex}\dot{m}_p \tag{1}$$

where m_p is the mass of propellant, $\dot{m}_p$ represents the mass variation in time, and v_{ex} is the exhaust velocity.

The specific impulse is defined by

$$Isp = \frac{T}{\dot{m}g} \tag{2}$$

where $\dot{m}$ is the xenon mass flow rate. Thus, the Tables 2 and 3 shows the values of these parameters for 150 V, and 300 V.

The efficiency of the thruster is given by

$$\eta_R = \frac{1}{2}\frac{T^2}{\dot{m}P} \tag{3}$$

where P is the power. In this equation the thrust is in units of mN, and the power is in units of KW. Equation 3 describes the proportion of the input propellant mass that is converted into ions and subsequently accelerates within the electric thruster.

The efficiency can be also computed by

$$\eta_A = \eta_u \cdot \eta_c \cdot \eta_E \tag{4}$$

where η_u is the efficiency of the propellant, given by

$$\eta_u = \frac{\text{extracted ion current}}{\text{ion current}} = \frac{I_i}{I_a} \tag{5}$$

where $I_a = \frac{\dot{m}}{m}$, η_c is the current efficiency defined by

$$\eta_c = \frac{\text{extracted ion current}}{\text{total discharge current}} = \frac{I_i}{I_T}, \tag{6}$$

and η_E is the energy efficiency is given by

$$\eta_{\mathrm{E}} = \frac{m_a \langle v\cos\theta\rangle^2}{2eV} \tag{7}$$

In a steady-state condition, these two efficiency analysis methods (η_R,η_A) should exhibit similar values [5].

Tables 2 and 3 show the numerical values of the performance parameters obtained for 150 V and 300 V, respectively. It is clear that all parameters are higher for the higher anode voltage, however, the power also increases, which is an important issue for small satellites in which there is limited power available.

Table 2. Performance parameters for 150 V.

Performance at 150 V	
Parameters	**CHT Values**
Thrust (mN)	21.250
Specific Impulse (s)	433.23
Power (W)	254.768
Efficiency (η_R)	17.9
Efficiency (η_A)	23.8

Table 3. Performance parameters for 300 V.

Performance at 300V	
Parameters	**CHT Values**
Thrust (mN)	46.012
Specific Impulse (s)	938.07
Power (W)	715.616
Efficiency (η_R)	30.1
Efficiency (η_A)	32.7

4 Conclusions

In this paper we performed numerical simulations of a cylindrical Hall thruster, which is an electric propulsion device for CubeSats, when compared to traditional Hall Thrusters, due to its smaller dimensions, and is designed specifically to operate at low power levels. Its geometry reduces susceptibility to channel wall erosion and makes it particularly suitable for low-power operations ($< 200W$) [7].

We compare the operational parameters of this thruster for two different values of the electrostatic potential at the anode, namely, 150 V and 300 V. Our numerical results indicate that the potential drop is primarily concentrated in the cylindrical section of the channel and into the plume. Two peaks in plasma density were observed: one in the annular region and the other at the axis further to the exit thruster ($x > 2.5cm$), which is attributed to the converging ion flux.

The efficiencies η_R and η_A showed proximity in the results. The first simulation (150V) exhibited a difference of 25%; however, for the second simulation (300V), there was a difference of 8%. These discrepancies are related to the averaging process during computation [5].

The performance of the CHT at 300 V displays higher values compared to the 150 V case. However, the power needed for the thruster also increases. The energy available at small satellites, and in CubeSats in particular, is very limited. Using permanent magnets for the generation of the magnetic field can reduce the power requirements of the CHT to the range of 50 - 300 W, compatible with that available for CubeSats. Since the power required for the 300 V configuration is outside this range, further work is needed to reduce the power needed while increasing the potential at the anode. Nevertheless, the analysis presented in this paper can be useful to decide which configuration is the most adequate, taking into account the power available of the propulsion system from a satellite power system.

Acknowledgements. The authors are grateful to the LAPLACE Laboratory at Toulouse for kindly making the HALLIS software available at `https://www.hallis-model.com`. RAM acknowledges support from DPI/DPG/UnB, and CNPq (Brazil) under award numbers 407493/2022-0 and 407341/2022-6, and FAP DF under award number 0193-00002206/2023-12. SGSPC acknowledges support from CAPES (Brazil). HOCJ acknowledges support from FUB/DPI/COPEI under award number 7178.

References

[1] D. M. Goebel. *Fundamentals os Eletric Propulsion: Ion and Hall Thrusters*. New Jersey: John Wiley & Sons, 2008.
[2] Y. Raitses and N. Fisch. Parametric investigations of a nonconventional hall thruster. *Physics of Plasmas*, vol. 8, n. 5, pp. 2579–2586, 2001.
[3] R. A. Miranda, A. A. Martins, and J. L. Ferreira. Particle-in-cell numerical simulations of a cylindrical hall thruster with permanent magnets. *Journal of Physics: Conference Series*, vol. 911, pp. 012021, 2017.
[4] M. Seo, J. Lee, J. Seon, H. June Lee, and W. Choe. Effect of the annular region on the performance of a cylindrical hall plasma thruster. *Physics of Plasmas*, vol. 20, n. 2, pp. 023507, 2013.
[5] I. Laplace. Hybrid model of hall ion sources. https://www.hallis-model.com/, 2018.
[6] G. J. M. Hagelaar, J. Bareilles, L. Garrigues, and J. P. Boeuf. Two-dimensional model of a stationary plasma thruster. *Journal of Applied Physics*, vol. 91, n. 9, pp. 5592–5598, 2002.
[7] L. Garrigues, G. Hagelaar, J. Boeuf, Y. Raitses, A. Smirnov, and N. Fisch. Simulations of a miniaturized cylindrical hall thruster. *IEEE Transactions on Plasma Science*, vol. 36, n. 5, pp. 2034–2042, 2008.